HHS Public Access

Author manuscript

Neuropsychopharmacology. Author manuscript; available in PMC 2011 February 01.

Published in final edited form as:

Neuropsychopharmacology. 2010 August ; 35(9): 1897–1909. doi:10.1038/npp.2010.61.

Calcium/calmodulin dependent protein kinase II mediates hippocampal glutamatergic plasticity during benzodiazepine withdrawal

Guofu Shen[1], **Bradley J. Van Sickle**[1], and **Elizabeth I. Tietz**[1,2]

[1]Department of Physiology and Pharmacology, University of Toledo College of Medicine, Health Science Campus, Toledo, OH, 43614

[2]Department of Neurosciences, University of Toledo College of Medicine, Health Science Campus, Toledo, OH, 43614

Abstract

Benzodiazepine withdrawal-anxiety is associated with potentiation of α-amino-3-hydroxy-5-methyl-4-isoxazolepropionate receptor (AMPAR) currents in hippocampal CA1 pyramidal neurons attributable to increased synaptic incorporation of GluA1-containing AMPARs. The contribution of calcium/calmodulin dependent protein kinase II (CaMKII) to enhanced glutamatergic synaptic strength during withdrawal from 1-week oral flurazepam (FZP) administration was further examined in hippocampal slices. As previously reported, AMPAR-mediated miniature excitatory postsynaptic current (mEPSC) amplitude increased in CA1 neurons from 2-day, but not 1-day FZP-withdrawn rats, along with increased single-channel conductance estimated by NSNA. Input-output curve slope was increased without a change in paired-pulse facilitation, suggesting increased AMPAR postsynaptic efficacy rather than altered glutamate release. The increased mEPSC amplitude and AMPAR conductance were related to CaMKII activity, as intracellular inclusion of CaMKIINtide or autocamtide-2 related inhibitory peptide (AIP), but not scrambled peptide, prevented both AMPAR amplitude and conductance changes. mEPSC inhibition by 1-naphthyl acetyl spermine and the negative shift in rectification index at both withdrawal time-points were consistent with functional incorporation of GluA2-lacking AMPARs. GluA1, but not GluA2 or GluA3 levels were increased in immunoblots of postsynaptic density (PSD)-enriched subcellular fractions of CA1 minislices from 1-day FZP-withdrawn rats, when mEPSC amplitude, but not conductance was increased. Both GluA1 expression levels and CaMKIIα–mediated GluA1 Ser^{831}-phosphorylation were increased in PSD-subfractions from 2-day FZP-withdrawn rats. Since phospho-Thr^{286}CaMKIIα was unchanged, CaMKIIα may be activated via an alternative signaling pathway. Synaptic insertion and subsequent CaMKIIα-mediated Ser^{831} phosphorylation of GluA1 homomers contribute to benzodiazepine withdrawal-

*Corresponding Author: Elizabeth I. Tietz, Ph.D., Department of Physiology and Pharmacology, University of Toledo College of Medicine, University of Toledo Health Science Campus, (formerly Medical University of Ohio), 3000 Arlington Ave., Mailstop 1008, Toledo, OH 43614, Tel: (419) 383-4170; Fax: (419) 383-2871, liz.tietz@utoledo.edu.

Disclosure/Conflict of Interest: The authors declare that, except for income receive from our primary employers, no financial support or compensation has been received from any individual or corporate entity over the past three years for research or professional service and there are no personal financial holdings that could be perceived as constituting a potential conflict of interest.

induced AMPAR potentiation and may represent an important hippocampal pathway mediating both drug-induced and activity-dependent plasticity.

Keywords

CA1 neuron; CaMKII; AMPA receptor; GluA subunits; GluR subunits; drug dependence

Introduction

Benzodiazepines, allosteric modulators of the $GABA_A$ receptor, are a safe, well-tolerated and effective treatment for anxiety, insomnia and seizures, yet carry some abuse liability and signs of physical dependence may emerge after long-term use (Griffiths and Johnson, 2005). While benzodiazepine tolerance has been associated primarily with $GABA_A$ receptor regulation (Bateson, 2002), mechanisms involving both GABAergic and glutamatergic systems have been proposed to underlie manifestations of benzodiazepine dependence (Allison and Pratt, 2003; Wafford, 2005). In fact, pharmacological approaches using specific glutamate receptor antagonists to modify withdrawal phenomena suggested that activation of excitatory amino acid receptors might be central to the expression of benzodiazepine physical dependence (Dunworth and Stephens, 1998; Koff *et al*, 1997; Van Sickle *et al*, 2004; Xiang and Tietz, 2007).

Abrupt withdrawal from prolonged benzodiazepine administration results in potentiation of alpha-amino-3-hydroxy-5-methyl-4-isoxazolepropionate receptor (AMPAR)-mediated synaptic currents associated with withdrawal-anxiety (Van Sickle and Tietz, 2002b; Xiang and Tietz, 2007). The amplitude of AMPAR-mediated miniature (m)EPSCs was progressively increased in hippocampal CA1 pyramidal neurons from 1-day and 2-day flurazepam (FZP)-withdrawn rats associated with a localized increase in AMPAR binding (Van Sickle *et al*, 2002b; Van Sickle *et al*, 2004) and an increase in glutamate efficacy (Song *et al*, 2007). Immunofluorescence and immunoblot studies revealed that GluA1 (GluR1, Collingridge *et al*, 2009), but not GluA2 (GluR2) subunit expression coupled with the enhancement of the GluA1 scaffolding protein, synapse associated protein 97 (SAP97) may be responsible for the enhanced glutamate-elicited currents in CA1 neurons (Song *et al*, 2007; see also Izzo *et al*, 2001). The latter interpretation was further supported using postembedding immunogold electron microscopy (EM). GluA1, but not GluA2 immunoreactivity was increased at CA1 neuron asymmetric synapses (Das *et al*, 2008).

The GluA1 subunit, one of two major hippocampal AMPAR subunits, has a long cytoplasmic carboxyl terminus, which undergoes phosphorylation by several kinases. GluA1 trafficking and phosphorylation contribute to activity-dependent synaptic plasticity (Derkach *et al*, 2007). In particular, a transient increase in GluA1 AMPARs (Plant *et al*, 2006) was detected as both a shift in the current rectification index in the presence of spermine analogues (Washburn and Dingledine, 1996) and by an alteration in AMPAR single-channel properties (Benke *et al*, 1998; Luthi *et al*, 2004). Calcium/calmodulin dependent protein kinase II (CaMKII), one of the most abundant proteins in the postsynaptic density (PSD), is required for activity-dependent membrane incorporation of GluA1 (and GluA4) subunit-

containing AMPARs (Esteban *et al*, 2003), and subsequent phosphorylation of GluA1-subunits at Ser^{831} enhancing single-channel conductance of GluA2-lacking AMPARs (Derkach *et al*, 1999; Oh and Derkach, 2005).

To further explore the contribution of CaMKII to AMPAR potentiation during benzodiazepine withdrawal, whole-cell mEPSCs were recorded in CA1 pyramidal neurons in hippocampal slices from rats withdrawn from 1-week oral flurazepam (FZP) administration to evaluate AMPAR-mediated synaptic transmission and single-channel conductance by non-stationary noise analysis (NSNA). Input-output (I/O) relationships and paired-pulse facilitation (PPF) were used in conjunction to assess the contribution of pre- and postsynaptic mechanisms to enhanced AMPAR currents. A potent spermine analogue was applied extracellularly to evaluate the contribution of GluA2-lacking, Ca^{2+}-permeable receptors (Pellegrini-Giampietro, 2003; Washburn and Dingledine, 1996) to the transient, progressive, increase in AMPAR potentiation during benzodiazepine withdrawal. Intracellular application of active and inactive CaMKII inhibitors was used to evaluate the role of CaMKII to modify AMPAR conductance. Immunoblots of PSD-enriched subcellular fractions of CA1 minislices were used to evaluate the withdrawal-associated expression patterns of total and phosphorylated GluA1-3 and CaMKIIα/β subunits. The findings suggest that insertion of GluA1 homomeric AMPARs and CaMKII-mediated phosphorylation of Ser^{831}GluA1 coupled with enhanced hippocampal AMPAR conductance may represent one common feature among drug-induced and other activity-dependent models of plasticity.

Materials and Methods

FZP-withdrawal Model

A FZP dosing regimen was used which reliably induces manifestations of both benzodiazepine tolerance and dependence in both juvenile and adult rats (Song *et al*, 2007; Van Sickle and Tietz, 2002b; Van Sickle *et al*, 2004; Zeng and Tietz, 1999). Male Sprague-Dawley rats (Harlan, Indianapolis, IN), postnatal day (PN) 36-42 at the time of study were handled in accordance with institutional and NIH guidelines and approved by the University of Toledo Institutional Animal Care and Use Committee. Rats were first adapted to the animal facility and to the 0.02% saccharin vehicle for 2-4 days, then offered FZP (provided by the National Institute of Drug Abuse Supply Program) in 0.02% saccharin vehicle for 1 week (100 mg/kg × 3 days; 150 mg/kg × 4 days) as their sole source of drinking water, followed by 1 or 2 days of drug withdrawal. Daily water consumption was monitored to adjust the drug concentration to offer the desired dose. Rats that did not reach a weekly average of 120 mg/kg/day were excluded. FZP-treated rats received saccharin water during the withdrawal period. Matched control rats received the saccharin vehicle in parallel throughout the course of study. All electrophysiological and immunochemical studies described were conducted with the experimenter blind to the experimental treatment groups.

Hippocampal Slice Preparation

Following decapitation, the hippocampus was rapidly dissected and transverse dorsal hippocampal slices (400 μm) were cut on vibratome (Ted Pella, Redding CA) in ice-cold,

pre-gassed, low-calcium artificial cerebrospinal fluid (ACSF) containing (in mM): NaCl 120; KCl 2.5; $CaCl_2$ 0.5; $MgCl_2$ 7.0; NaH_2PO_4 1.2; $NaHCO_3$ 2; D-glucose 20; ascorbate 1.3; pH 7.4. Slices were maintained at room temperature (22°C) for 15 min in gassed low-calcium ACSF and then transferred to normal ACSF containing (in mM): NaCl 119; KCl 2.5; $CaCl_2$ 1.8; $MgSO_4$ 1.3; NaH_2PO_4 1.25; $NaHCO_3$ 26; D-glucose 10; pH 7.4. Slices recovered at room temperature for ≥ 2 hr in ACSF prior to electrophysiological recording. During recording, slices were perfused at a rate of 2.5 ml/min with gassed ACSF at room temperature.

Whole-cell Electrophysiological Recording

For whole-cell AMPAR-mediated mEPSC recordings, hippocampal slices were continuously perfused with oxygenated ACSF and visualized on an upright Zeiss Axioskop. Blind whole-cell patch-clamp recordings from CA1 pyramidal neurons were made using borosilicate micropipettes (4-7 MΩ, WPI, Sarasota, FL) containing (in mM): Cs methanesulfonate 132.5; CsCl 17.5; HEPES 10; EGTA 0.2; NaCl 8; Mg-ATP 2; Na_3-GTP 0.3; QX-314 2; pH 7.2. Alternately, the CaMKII inhibitor autocamtide-2, a CaMKII substrate (H-KKALRRQETVDAL-OH, 5 μM, EMD Chemicals, Madison, WI) or the more potent, selective CaMKII inhibitor (Ishada *et al*, 1995) autocamtide-2 inhibitory peptide (H-KKKLRRQEAFDAL-OH, AIP, 5 μM, EMD Chemicals) was added to the micropipette prior to mEPSC recordings. A control scrambled peptide (H-ELRKFQADLKRKA-OH) used at the same micropipette concentration was designed to disrupt both the basic C-terminal and hydrophobic N-terminal groups of AIP. The scrambled sequence was analyzed online using the blastp (protein-protein) suite in the National Center for Biotechnology Information (NCBI) BLAST tool (http://blast.ncbi.nlm.nih.gov/Blast.cgi) and no similar sequence was found in the current database. Since it was more recently shown that CaMKI (Guire *et al*, 2008), as well as CaMKII (Esteban et al, 2003) can recruit AMPARs to the synapse, the intracellular effects of the most selective CaMKII inhibitor available, CaMKIINtide (5 μM, Sanhueza *et al*, 2007) was also evaluated in several neurons from control and 2-day FZP-withdrawn rats. EPSCs were recorded under voltage clamp (V_H = -80 mV) in the presence of 1 μM tetrodotoxin (TTX, Alomone Labs, Jerusalem, Israel), 50 μM APV (Tocris Bioscience, Ellisville, MO), 50 μM picrotoxin (Sigma-Aldrich, St. Louis, MO) and 25 μM CGP-35348 (Tocris) in ACSF. Signals were amplified with an Axoclamp2A amplifier coupled to a 4-pole Bessel filter/amplifier (1 kHz, 100×, Cornerstone) and digitized online (20 kHz, Digidata 1200A, Axon), then stored on computer disk for later analysis.

Non-stationary noise analysis—AMPAR single-channel conductance was estimated by offline non-stationary noise analysis (NSNA) of mEPSCs using MiniAnalysis 6.0 (Synaptosoft, Inc, Decatur, GA). Miniature events were detected over 10 min (1-day) or 20 min (2-day) recording. As reported previously, only fast events (10-90% rise time ≤ 3 ms) ≥ 8 pA were used (Shen *et al*, 2009). All selected events were baseline-adjusted, peak-scaled, superimposed and compared to the peak-scaled mean. The variance of amplitudes during the decay phase was plotted against mean amplitude of mEPSC currents and fitted with the equation: $\sigma^2 = i^* I - I^2/N$ where σ^2 is the variance of the mEPSC, *i* indicates the unitary current, I represents the mean of whole-cell current, and N is the total number of channels.

The single-channel conductance was calculated by Ohm's law: $\gamma = i/(V_H - V_{rev})$, where V_H is −80 mV and V_{rev} of AMPAR currents was 0 mV.

Input/output relationship—Evoked AMPAR-mediated EPSCs (eEPSCs, V_H=-80 mV) were induced in the absence of TTX, with a bipolar stimulating electrode placed in the Schaffer collateral pathway. I/O curves were constructed by varying stimulus intensity (V) and measuring peak ESPC current amplitude (pA) from EPSC threshold to spike threshold. The slope of both mean and individual I/O curves was calculated to estimate synaptic efficacy of AMPAR responses.

Paired-pulse facilitation—Stimulus intensity was then adjusted to induce half-maximal responses and paired-pulses were delivered at intervals from 25 ms to 200 ms in 25 ms increments. Paired-pulses were elicited at a frequency of 0.16 Hz. Peak amplitude for individual, paired-pulse responses was measured as the difference between the baseline before the stimulus artifact and the peak eEPSC. PPF was calculated as $(EPSC_2\text{-}EPSC_1)/EPSC_1 \times 100$.

Spermine analogue inhibition—Three AMPAR subpopulations are primarily expressed in rat hippocampus, GluA1/2 and GluA2/3 heteromers, and to a lesser extent GluA1 homomers (Moga *et al*, 2003; Wenthold *et al*, 1996). Heteromeric GluA2-containing AMPARs exhibit low permeability for divalent cations such as Ca^{2+}, whereas GluA2-lacking receptors have high divalent cation permeability (Hollmann *et al*, 1991). Furthermore, GluA2-containing and GluA2-lacking AMPARs also differ in their pharmacological properties, in particular blockade by extracellularly applied polyamine-containing spider and wasp toxins (Washburn and Dingledine, 1996). To evaluate whether GluA2-lacking receptors were present at CA1 neurons synapses during FZP-withdrawal, 100 μM 1-naphthyl acetyl spermine (NAS, Sigma-Aldrich, St. Louis, MO) was added to the perfusate in the presence of 10 μM APV during AMPAR-mediated (V_H=-80 mV) mEPSC recordings before (10 min) and after (7 min) NAS application. Mean mEPSC amplitude was measured before and after NAS application and the percentage decrease after NAS was calculated.

Furthermore, GluA2-containing AMPARs show linear current-voltage (I-V) relationships or outward rectification, whereas GluA2-lacking AMPAR subunits are prone to spermine blockade and show inward rectification at positive holding potentials (Washburn and Dingledine, 1996). Analogous to recordings in 2-day FZP-withdrawn rats (Song *et al*, 2007), rectification studies were carried out in hippocampal slices from 1-day FZP withdrawn rats with 100 μM spermine in the micropipette. The rectification index was defined as peak current amplitude at a holding potential of +40 mV divided by that at -60 mV.

Immunoblot Analyses of CA1 Minislices

Subcellular fractionation—For immunoblotting, hippocampi were isolated from 3 matched pairs of control and FZP-withdrawn rats and pooled (21 rats/group; n = 7 wells/group; 2-day GluA1 33 rats/group, n = 11 wells/group; GluA3 (GluR3) and CaMKIIβ 12 rats/group; n = 4 wells/group). The CA1 region was microdissected from the whole

hippocampus, then homogenized and centrifuged to obtain a cytosolic fraction (S2), crude membrane pellet (P2) and a PSD-enriched subfraction as previously described (Song *et al*, 2007). All procedures were conducted at 0-4°C.

Immunoblotting—Protein (15 μg/well) was separated by 10% SDS-PAGE and wet-transferred to nitrocellulose. Primary antibodies anti-GluA1 (1:2,000, Millipore, Billerica, MA), anti-phopho-Ser^{831}-GluA1 (1:1,000, Millipore), anti-GluA2 (1:2,000, Millipore), anti-GluA3 (1:100, Millipore,), anti-CaMKIIα (1:5,000, Millipore), anti-phospho-Thr^{286}-CaMKII (1:1,000, Promega Corporation, Madison, WI), anti-CaMKIIβ (1:1,000, Abcam Inc., Cambridge, MA), anti-actin (1:50,000, Millipore) or anti-GAPDH (1:20,000, Abcam Inc.) were incubated with membranes overnight at 4°C. Antibody signals were detected with anti-rabbit or anti-mouse horseradish peroxidase (HRP)-conjugated secondary antibodies (1:10,000, Jackson ImmunoResearch, West Grove, PA), followed by enhanced chemiluminescence (ECL) (Denville Scientific, Metuchen, NJ). Images of immunoblots were scanned and immunoreactivity quantified with ImageJ software, v. 1.36b (National Institutes of Health, Bethesda, MD). GluA or CaMKII subunit signals were normalized to the corresponding GAPDH or actin signal.

Results

Postsynaptic Mechanisms of AMPAR Potentiation during Benzodiazepine Withdrawal

As previously reported (Van Sickle and Tietz, 2002b; Xiang and Tietz, 2007), the amplitude of AMPAR-mediated mEPSCs was significantly increased in CA1 neurons from 2-day FZP-withdrawn rats without effect on mEPSC frequency, rise-time or decay kinetics or resting membrane potential (RMP). I/O experiments confirmed an increased efficacy of synaptic transmission in CA1 neurons from FZP-withdrawn rats. As shown in Fig. 1A, an I/O curve generated by plotting mean evoked EPSC amplitude (pA) versus mean stimulus intensity (V), showed a ∼2.5 fold increase in slope. A similar result (Fig. 1B) was obtained when comparing the mean slope of fits of individual I/O curves (CON, 205.3 ± 44.5 pA/V vs. FZP, 440.0 ± 79.4 pA/V, $p<0.05$). The potentiation of AMPAR-mediated synaptic transmission reflected in the enhanced slope of the FZP-withdrawn I/O curve paralleled an increase in population spike amplitude (Shen *et al*, 2009) and in overall CA1 neuron hyperexcitability (Van Sickle *et al*, 2004) in FZP-withdrawn neurons.

Although mEPSC frequency, which reflects random release of glutamate from presynaptic neurons was not different between groups (Van Sickle and Tietz, 2002b; Van Sickle *et al*, 2004; Shen *et al*, 2009), paired-pulse facilitation (PPF) studies were carried out to verify that evoked glutamate release was also not affected during drug withdrawal. Maximal facilitation was observed at the shortest interstimulus interval tested (25 ms) and decayed exponentially with increasing interstimulus intervals (25-200 ms). Consistent with the enhancement of synaptic efficacy in FZP-withdrawn neurons, FZP half-maximal responses tended to be greater than in control rats, yet there were no significant differences in the half-maximal response (CON: 171.5 ± 41.6 pA vs. FZP: 314.3± 69.6 pA, n = 5/group, p = 0.12) or stimulus intensity (CON: 0.34 ± 0.09 V vs. FZP: 0.23 ± 0.04 V, n = 5/group, p = 0.28, Student *t*-test) used to elicit PPF. There were no significant differences (p=0.23 to 0.94)

among PPF responses between experimental groups at any interstimulus interval (Fig. 1C inset: representative traces), reflected in the overlap of the single-exponential decay fits (Fig. 1C). Taken together, the lack of change in mEPSC frequency and PPF, suggests that glutamate release was unchanged between experimental groups excluding presynaptic involvement in benzodiazepine withdrawal-induced AMPAR potentiation.

In models of activity-dependent plasticity, such as long-term potentiation (LTP), CaMKII is primarily activated by Ca^{2+} influx through N-methyl-D-aspartate receptors (NMDARs) (Collingridge *et al*, 2004) potentiates synaptic efficacy by inducing synaptic insertion of AMPARs, as well as increasing AMPAR single-channel conductance via CaMKII-mediated Ser^{831} GluA1 subunit phosphorylation (Lisman *et al*, 2002). AMPAR conductance in CA1 neurons from 2-day FZP-withdrawn rats nearly doubled, from 8.5 to 14.7 pS (Shen *et al*, 2009) an observation that resembled CaMKII-mediated phosphorylation of GluA1 subunits in LTP (Barria *et al*, 1997b) and modulation of AMPAR conductance in recombinant GluA1 homomeric AMPARs (Derkach *et al*, 1999). Since mEPSC amplitude was significantly increased in 1-day FZP-withdrawn rats (Van Sickle and Tietz, 2002), NSNA was also used to estimate single-channel conductance at this withdrawal time-point. Unlike in recordings from 2-day withdrawn rats, NSNA analysis of mEPSCs in CA1 neurons from control and 1-day FZP-withdrawn rats confirmed an enhanced AMPAR amplitude (Fig. 2A, CON, 9.4 ± 0.2 pA, n = 6 vs. FZP, 10.3 ± 0.3 pA, n = 7, p = 0.04), without a change in conductance level (Fig. 3B, CON, 11.0 ± 0.6 pS, n =6 vs. FZP, 11.8 ± 1.2 pS, n = 7)

The enhanced mEPSC amplitude and estimated single-channel conductance in CA1 neurons was consistent with previous findings from both juvenile and adult 2-day FZP-withdrawn rats (Van Sickle and Tietz, 2002, Van Sickle *et al*, 2004; Shen *et al*, 2009) and with a CaMKII-mediated mechanism regulating AMPAR potentiation during benzodiazepine withdrawal. Indeed, both effects were eliminated by preincubation (2 hr) of hippocampal slices with the CaMKII inhibitor, KN-93 (Shen *et al*, 2009). However, since bath-applied KN93 and KN92 can have presynaptic actions and also have effects on L-type voltage-gated Ca^{2+} channels (Gao *et al*, 2006), the postsynaptic effects of CaMKII on AMPAR potentiation were further evaluated by inclusion of the CaMKII inhibitors, AIP or ACM in the micropipette. sAIP, at the same concentration was used as a negative control. The effects of the more selective inhibitor, CaMKIINtide (Sanhueza *et al*, 2007) were also evaluated in several control and 2-day FZP-withdrawn neurons. A comparison between neurons recorded in ACSF without sAIP in the micropipette (n=9 cells/ experimental group, Shen *et al*, 2009) and those in the present study (Table 1) did not reveal any significant differences among control group values. Inclusion of the active peptide, AIP blocked AMPAR potentiation (Fig. 3 and Table 1). That is, both the increased AMPAR-mediated mEPSC amplitude and AMPAR single-channel conductance in neurons from 2-day FZP-withdrawn rats returned to control levels. As shown in Fig. 3 and Table 1, intracellular application of sAIP had no significant effect on mEPSC amplitude (Fig. 3A) or single-channel conductance (Fig. 3C) in FZP-withdrawn vs. control neurons in which mEPSCs remained significantly increased. The estimated single-channel conductance derived from a representative set of recordings from each experimental group is shown in Fig. 3B. The effect of the less-potent CaMKII inhibitor, ACM did not reach statistical significance (Table 1). As with AIP, intracellular

inclusion of CaMKIINtide prevented both the increase in peak amplitude (CON: 9.3 ± 1.1 pA, n = 4; FZP: 10.1 ± 2.4 pA, n= 3, p = 0.58) and estimated conductance (CON: 8.9 ± 0.5 pS, n = 4; FZP: 9.6 ± 0.2 pS, n= 3, p = 0.76) without an effect on RMP, rise-time, or tau of decay.

GluA2-lacking Receptors Mediate AMPAR Potentiation

Since the number of AMPAR binding sites and of GluA1-, but not GluA2-containing AMPARs was increased at CA1 neuron synapses in FZP-withdrawn rats (Das *et al*, 2008; Song *et al*, 2007; Van Sickle and Tietz, 2002b), an enhancement in AMPAR current amplitude was proposed to be due to an increase in the numbers of GluA2-lacking AMPAR numbers. Inward rectification in the presence of spermine or its analogs was therefore used as an electrophysiological tag for the detection of Ca^{2+}-permeable, GluA2-lacking AMPAR (Derkach *et al*, 1999). mEPSCs recorded from CA1 neurons in hippocampal slices from FZP-withdrawn rats showed a decreased +40/-60 rectification index with 100 μM spermine in the micropipette (Song *et al*, 2007). A similar effect on rectification index was observed in neurons evaluated from 1-day FZP withdrawn rats (FZP, 0.56 ± 0.05, n= 8; CON, 0.81 ± 0.06, n=8, p <0.01). Furthermore as illustrated by its effect on representative average mEPSCs (Fig. 4A and D), extracellular application of NAS, another selective inhibitor of AMPAR currents mediated by GluA2-lacking receptors, had a significantly greater effect to inhibit AMPAR-mediated mEPSC amplitude in CA1 neurons from 1 and 2-day FZP-withdrawn vs. control rats (Fig. 4B and E). Removing the synaptic current component mediated by Ca^{2+}-permeable AMPARs with NAS also abolished the potentiation of mEPSC amplitude in neurons from FZP-withdrawn rats (Fig. 4C and F) (1-day: FZP, 10.3 ± 0.3 pA vs. FZP + NAS, 8.3 ± 0.4 pA, n=7, p = 0.002; 2-day: FZP, 10.6 ± 0.3 pA vs. FZP + NAS, 8.4 ± 0.4 pA, n=12, p < 0.0001). The effect was might be smaller in control neurons since GluA1 homomers make up less than 10% of AMPARs (1-day: CON, 9.4 ± 0.2 pA vs. CON + NAS, 8.5 ± 0.2 pA, n=6, p = 0.01; 2-day: CON, 9.0 ± 0.3 pA vs. CON + NAS, 8.1 ± 0.4 pA, n=7, p = 0.10). This finding lent further support to the hypothesis that AMPAR potentiation during drug withdrawal was mediated by incorporation of GluA2-lacking AMPAR into CA1 neuron synapses.

Expression Pattern of GluA and CaMKII Subunits in PSD-enriched Subcellular Fractions

Electrophysiological findings in 1-day and 2-day FZP-withdrawn rats (Figs. 2 and 3, Van Sickle *et al*, 2004; Shen *et al*, 2009) suggested that synaptic incorporation of GluA1-containing AMPAR may mediate the increase in mEPSC amplitude and that subsequent CaMKII-mediated phosphorylation of Ser^{831}GluA1 may mediate enhanced AMPAR conductance. Therefore, total and phospho(p)Ser^{831}GluA1 subunit levels were examined by immunoblot analysis of subfractionated proteins in PSD-enriched subcellular fractions of CA1 minislices from 1-day and 2-day FZP withdrawn rats. GluA1 and pSer^{831}GluA1 expression levels in the cytosolic (S2) and crude membrane (P2) subfractions (data not shown) were unchanged after 2-day withdrawal. However, total GluA1 expression levels in the PSD-enriched subfraction were elevated in both 1-day and 2-day FZP-withdrawn subfractions (Fig. 5A and B), as reported previously after 2-days (Song *et al*, 2007). As in 2-day FZP-withdrawn tissues (Das *et al*, 2008; Song *et al*, 2007), GluA2 subunit protein levels were also unchanged in 1-day FZP-withdrawn subfractions (Fig. 5B). As shown in the lower

panels in Fig. 5B, pSer^{831}GluA1 subunit levels were elevated in PSD-enriched subfractions in 2-day, but not 1-day FZP-withdrawn subfractions (Fig. 5A), consistent with an increase in AMPAR conductance in neurons from 2-day (Fig. 3, Shen *et al*, 2009), but not 1-day FZP-withdrawn rats (Fig. 2).

The increased expression of GluA1 subunits in CA1 minislices from 1-day FZP-withdrawn rats provides support for the proposal that GluA1-containing AMPARs were incorporated into CA1 synapses prior to Ser^{831} phosphorylation by CaMKII resulting in a subsequent functional increase in AMPAR single channel conductance (Oh and Derkach, 2005). Nonetheless, benzodiazepine withdrawal-induced Ca^{2+}-permeable AMPAR complexes could include GluA1 and GluA3 homomers or additionally GluA1/GluA3 heteromers, a composition that cannot be pharmacologically distinguished by NAS-mediated blockade (Fig. 4). Thus as an initial step to distinguish among these possibilities, GluA3 subunit levels were also assessed in 2-day FZP-withdrawn minislices. Fig. 6B shows that GluA3 subunit levels were unchanged in the PSD-enriched subfraction from 2-day FZP-withdrawn minislices. These data suggest that GluA3-containing AMPAR did not contribute to the shift in inward rectification index (Song *et al*, 2007) or to enhanced Ca^{2+}-permeable AMPAR currents (Fig. 4), thus did not play a role to enhance excitatory synaptic transmission in FZP-withdrawn neurons. Taken together, these data provide further support for the interpretation that AMPAR potentiation is related to synaptic incorporation and phosphorylation of GluA1 homomers.

Because Ser^{831} GluA1 has been identified as a substrate of CaMKII (Barria *et al*, 1997a; Mammen *et al*, 1997) and can be phosphorylated by the constitutively active form, phospho(p)Thr^{286}-CaMKII, the expression levels of total- and pThr^{286}-CaMKII were also examined in all subfractions derived from 1-day and 2-day FZP-withdrawn minislices. Total CaMKII protein levels were significantly, and ubiquitously increased in all three subfractions (S2, P2: data not shown) and PSD-enriched subfractions from 2-day, but not 1-day FZP-withdrawn CA1 minislices (Fig. 6A and B) providing a possible mechanism for Ser^{831} phosphorylation of AMPAR GluA1 subunits at the latter withdrawal time-point. But unlike changes in pThr^{286}-CaMKII associated with LTP induction (Lisman *et al*, 2002; Bayer *et al*, 2006), expression levels of the constitutively active form of CaMKII were unchanged at both time-points after drug withdrawal (Fig. 6A and B). Since a small fraction of CaMKIIβ can dock the more prevalent, CaMKIIα to the actin cytoskeleton (Shen *et al*, 1998), CaMKIIβ levels were also compared in these PSD-enriched subfractions. There were no significant differences in CaMKIIβ expression in the PSD-enriched subfraction derived from 2-day FZP-withdrawn minislices (Fig. 6B).

Discussion

Enhanced AMPAR Postsynaptic Efficacy

A significant link was previously established between the increased efficacy of hippocampal CA1 pyramidal neuron AMPAR-mediated glutamatergic synaptic transmission and withdrawal-induced anxiety-like behavior (Van Sickle *et al*, 2004; Xiang and Tietz, 2007), consistent with findings in other benzodiazepine-withdrawal models (Allison and Pratt, 2003; Izzo *et al*, 2001) and other animal models of anxiety (Shen *et al*, 2007). The

enhancement of macroscopic glutamate currents and increased AMPAR-mediated mEPSC amplitude in the absence of a change in glutamate affinity or current desensitization was attributable to increased GluA1-, but not GluA2-containing AMPARs at CA1 neuron synapses (Das *et al*, 2008; Song *et al*, 2007). Along with previous findings in hippocampal slices (Van Sickle and Tietz, 2002; Van Sickle *et al*, 2004), the ∼2.5-fold increased slope of the I/O relationship confirmed that AMPAR-mediated synaptic transmission was potentiated in 2-day FZP-withdrawn rats (Fig. 1A and B). A similar effect was noted in lateral amygdala slices of fear-conditioned rats (McKernan and Shinnick-Gallagher, 1997). However, unlike in the latter model of emotional learning, presynaptic facilitation of glutamate release was not observed (Fig. 1C) and mEPSC frequency was unaltered in FZP-withdrawn rats (Shen *et al*, 2009; Van Sickle and Tietz, 2002; Van Sickle *et al*, 2004). In common with current views of mechanisms underlying LTP (Nicoll, 2003), a presynaptic mechanism is not likely central to drug-induced glutamatergic plasticity.

Though previous experiments showed that bath application of hippocampal slices with the CaMKII inhibitor, KN-93 could prevent AMPAR potentiation during 2-day FZP withdrawal (Shen *et al*, 2009), a presynaptic mechanism could not be excluded since CaMKII can also modulate neurotransmitter vesicle release (Llinas *et al*, 1985; Margrie *et al*, 1998). To rule out presynaptic effects of CaMKII inhibition, various CaMKII inhibitors were included in the micropipette. Intracellular inclusion of AIP, but not the scrambled peptide, as well as CaMKIINtide had a similar effect as the less selective bath-applied inhibitor to prevent potentiation of AMPAR synaptic currents and conductance (Shen *et al*, 2009). These findings provide strong evidence that postsynaptic CaMKII activation is involved in CA1 neuron hyperexcitability. As with LTP, enhancing CaMKIIα activity can lead to synaptic delivery of GluA1-containing AMPARs, an increase in mEPSC quantal size and enhanced AMPAR conductance in hippocampal neurons and heterologous systems (Poncer *et al*, 2002; Oh and Derkach, 2005). Accordingly, an increase in trafficking and subsequent CaMKII-mediated phosphorylation of GluA1-containing AMPARs (Barria *et al*, 1997b; Derkach *et al*, 1999; Esteban *et al*, 2003; Hayashi *et al*, 2000) offered a possible molecular basis for synaptic AMPAR potentiation associated with benzodiazepine withdrawal.

Incorporation of homomeric GluR1 AMPAR

GluA1/2 heteromers represent a large portion (∼80%) of native synaptic CA1 neuron AMPARs and GluA2/3 heteromers a dominant fraction of the remainder (Lu *et al*, 2009; Wenthold *et al*, 1996). GluA1/3 heteromers are rare in the presence of GluA2 subunits (Moga *et al*, 2003; Sans *et al*, 2003; Wenthold *et al*, 1996). GluA4 (GluR4) subunit expression is largely confined to the first postnatal week (Zhu *et al*, 2000). A small proportion (∼8%) of native AMPAR complexes were proposed to exist as GluA1 homomers (Wenthold *et al*, 1996), the small number of CA1 GluA1 homomers resides intracellularly or on non-pyramidal neurons. The intracellular subpopulation is trafficked to the CA1 synapse immediately upon a reduction in GluA2 expression (Lu *et al*, 2009). Q/R site editing, complete (>99%) at all stages of development (Seeburg, 1996) renders AMPAR containing even a single GluA2 subunit Ca^{2+} impermeable and insensitive to spermine block, while GluA2-lacking AMPARs show inward rectification (Pellegrini-Giampietro, 2003; Washburn and Dingledine, 1996, Swanson et al., 1997). Native CA1 neurons exhibit largely linear to

outward rectification in response to AMPA (Lerma *et al*, 1994; Song *et al*, 2007). The shift in the rectification index in 2-day FZP-withdrawn neurons (Song *et al*, 2007) was supportive evidence for functional incorporation of synaptic Ca^{2+} permeable GluA1-containing AMPARs (Esteban *et al*, 2003; Shi *et al*, 1999), though could not exclude an increase in GluA3 homomers or GluA1/3 heteromers (Moga *et al*, 2003; Pellegrini-Giampietro, 2003). The lack of change in GluA3 expression (Fig 5B) in 2-day withdrawn CA1 PSD-subfractions added support for the interpretation that GluA1-homomers are incorporated into excitatory synapses. The significant increase in spermine analogue (NAS) inhibition of mEPSCs in both 1-day and 2-day FZP-withdrawn neurons (Fig. 4) also supported an increased proportion of incorporation of GluA2-lacking AMPARs, rather than GluA1/2 heteromers into CA1 synapses at both withdrawal time-points.

A Two-Step Process: GluR1 Subunit Incorporation and Phosphorylation

AMPA receptors in CA1 neurons have multiple conductance states (Benke *et al*, 1998; Swanson *et al*, 1997). AMPAR conductance (γ) at CA1 synapses was estimated to be 7.7 pS, the range (1.5 to 22.3 pS, PN13-15) related to synaptic variation. Glutamate has concentration-dependent effects to increase AMPAR channel conductance (Gebhardt and Cull-Candy, 2006) and synaptic concentrations (1 mM) applied to outside-out CA1 dendritic patches revealed a mean conductance of 10.2 pS, despite their low calcium permeability ($P_{Ca2+/Cs+}$ ~0.5) (Spruston *et al*, 1995, PN13-28). Very low conductance channels (~300 fS), attributable to fully RNA-edited GluA2-containing receptors in native assemblies (Seeburg, 1996) reduced the weighted mean conductance (Swanson *et al*, 1997). GluA2-containing receptors expressed in HEK-293 cells had conductances of ~2-3 pS (Oh and Derkach, 2005). while 9 and 14 pS conductance states dominated GluA1 homomers, representing 85% of channel openings. Co-expression of CaMKII, GluA1 Ser^{831} phosphorylation or mutation of Ser^{831} to Asp, increased the occurrence of far less frequent, higher conductance states (21 and 28 pS, Derkach *et al.*, 1999, Oh and Derkach, 2005). Importantly, the latter increased GluA1 conductance was only functionally expressed in the *absence* of assembled GluA2 subunits (Oh and Derkach, 2005). These findings imply that a subpopulation of primarily Ca^{2+} impermeable GluA2-containing AMPARs, including extrasynaptic somatic receptors (Lerma, *et al*, 1994; Lu *et al*, 2009) with lower conductance states offsets a mixed population of higher conductance state dendritic AMPARs, each making a contribution to the whole-cell weighted mean conductance (Benke *et al*, 1998; Spruston *et al*, 1995).

The mean conductance derived from NSNA analysis of mEPSCs in CA1 neurons from control and 2-day FZP-withdrawn rats (Table 1, PN36-42), was comparable to that previously observed in this model (Shen *et al*, 2009). Since GluA1, but not GluA2 subunit expression was not increased in 1-day FZP-withdrawn rats (Fig. 5) and glutamate affinity was unchanged during FZP withdrawal (Song *et al*, 2007), the increased mEPSC amplitude likely reflected the increased insertion of homomeric GluA1-containing AMPARs at CA1 neuron synapses (Das *et al*, 2008). If a small number of newly contributing GluA1 homomers with a higher conductance state (9-14 pS, Derkach *et al*, 1999) were inserted into the synapse, this might result in the small, but significant increase in current amplitude without an observable change in the estimated conductance of native receptors in 1-day

FZP- withdrawn compared to matched control rats (Benke *et al*, 1998; Spruston *et al*, 1995). Furthermore, the evidence suggests that CaMKII phosphorylation of GluA1 Ser^{831} was responsible for the near doubling of estimated channel conductance observed in neurons from 2-day FZP-withdrawn rats (Fig. 6, Table 1).

Interestingly, in a model of CaMKII-mediated AMPAR recruitment, Guire *et al* (2008) calculated that for a typical CA1 hippocampal synapse containing ∼90 GluA2-containing AMPARs, recruitment and phosphorylation of just four GluA1 homomers was sufficient to increase synaptic strength by 80%. Since the number of AMPAR at the CA1 postsynaptic density was estimated to be ∼58-70 (Spruston *et al*, 1995), the 51-73% increase in synaptic strength associated with benzodiazepine withdrawal-anxiety would be consistent with the observed incorporation of GluA1, but not GluA2 subunits into CA1 neuron synapses (Das *et al*, 2008), and based on the latter model of AMPAR potentiation (Guire *et al*, 2008) would represent incorporation of just ∼2-3 GluA homomeric receptors/synapse (Shen *et al*, 2009). Collectively, the functional data suggested that AMPAR potentiation may be modified in a stepwise fashion during drug withdrawal, involving the progressive insertion of GluA1 homomers in 1-day FZP-withdrawn rats, possibly via PKA-mediated phosphorylation of Ser^{845} (Lee *et al*, 2010; He *et al*, 2009; Esteban *et al*, 2003; Song and Tietz, 2004), followed by enhanced GluA1 phosphorylation of Ser^{831} and a shift toward higher AMPAR conductance states on day 2 after withdrawal (Derkach et al., 1999; Esteban *et al*, 2003; Oh and Derkach, 2005).

To provide further insight into possible mechanisms by which AMPAR currents were potentiated during the withdrawal phase, the time-course of GluA and CaMKII subunit expression patterns and their relevant phospho- analogues was evaluated in PSD-enriched subfractions of CA1 minislices. Since GluA1, but not GluA2 or GluA3 subunit expression was enhanced (Fig. 5, see also Izzo *et al*, 2001), the immunoblot findings were consistent with the hypothesis that GluA1 homomers were incorporated into CA1 neurons from 1-day FZP-withdrawn rats, leading to increased AMPAR current amplitude, similar to that observed with LTP (Lledo *et al*, 1995; Barria et al., 1997b; Benke *et al*, 1998; Plant *et al*, 2006), though see also Adesnik and Nicoll, 2007). Interestingly, early LTP induced by theta burst stimulation was not maintained in slices from 2-day FZP-withdrawn rats, though behavioral effects on novel object recognition, and place and contextual memory were not observed (Shen *et al*, 2009). Since AMPAR potentiation was also mutually occluded by CaMKII activation or tetanic stimulation (Lledo *et al*, 1995; Wang and Kelly, 1995), the latter finding further suggests that LTP- and drug-induced plasticity may share a similar downstream CaMKII-mediated pathways.

Convergence/Divergence of Plasticity Models

The mechanisms by which AMPAR currents are potentiated during drug withdrawal and with other models of activity-dependent plasticity show numerous common features, though some notable dissimilarities. Unlike LTP, in which autophosphorylation of Thr^{286} leads to constitutive activation of CaMKIIα without a change in total CaMKIIα expression (Barria *et al*, 1997b; Lisman *et al*, 2002), $pThr^{286}$-CaMKII levels remained unchanged in PSD-enriched subfractions derived from 1-day or 2-day FZP-withdrawn rats. On the contrary, the

total CaMKIIα expression level was enhanced in all subcellular fractions from 2-day FZP-withdrawn rats (Fig. 6), while CaMKIIβ expression was unchanged in the PSD-enriched subfraction. Phosphorylation of Ser^{831}GluA1, in the face of enhanced CaMKIIα levels suggests that CaMKIIα levels in drug-withdrawn neurons might be autonomously-activated through an alternate mechanism, e.g. binding to the GluN2B subunit (Bayer *et al*, 2001, Bayer *et al*, 2006). Notably, expression of withdrawal-anxiety can be modulated in 2-day FZP-withdrawn rats via depression of NMDAR function (Van Sickle *et al*, 2002; Van Sickle *et al*, 2004). Moreover, preliminary immunoblot and EM findings indicate that depression of NMDAR function involves a reduction in GluN1/GluN2B receptors at CA1 neuron synapses (Shen *et al*, 2008; Das *et al*, 2009). Distinct from NMDAR-dependent LTP, in which Ca^{2+} influx primarily through NMDAR initiates CaMKII activation and AMPAR potentiation (Barria *et al*, 1997b, Collingridge *et al*, 2004), Ca^{2+} entry during benzodiazepine withdrawal may primarily occur via an increase in high voltage-activated Ca^{2+} channel current density (Katsura *et al*, 2007; Van Sickle *et al*, 2004; Xiang *et al*, 2008; Xiang and Tietz, 2007) and perhaps subsequently, via the increased density of Ca^{2+}-permeable, GluA1 homomeric AMPARs (Das *et al*, 2008; Song *et al*, 2007).

The findings in benzodiazepine-withdrawn rats extend previous studies, which reported that regulation of GluA1-containing AMPARs plays a significant role in a variety of models of drug-induced plasticity associated with drug abuse (Loweth *et al*, 2010; Anderson *et al*, 2008; Kauer and Malenka, 2007; Boudreau and Wolf 2005; Wolf *et al*, 2004; Sutton *et al*, 2003; Fitzgerald *et al*, 1996). GluA1 subunit alterations were detected in the mesolimbic dopamine reward system including prefrontal cortex and related limbic areas such as hippocampus and amygdala following withdrawal from repeated administration of a variety of drugs of abuse including opioids, cocaine and ethanol (Ortiz *et al*, 1995; Glass *et al*, 2005, 2008; Ghasemzadeh *et al*, 2009; Edwards *et al*, 2009;). For instance, behavioral sensitization which develops during withdrawal from repeated cocaine administration was recently associated with enhanced surface GluA1 expression in nucleus accumbens, without increased phospho-CaMKIIα levels (Boudreau *et al*, 2009), consistent with the observation that $pThr^{286}$-CaMKII expression was unchanged during benzodiazepine withdrawal, despite enhanced GluA1 homomer Ser^{831} phosphorylation. Moreover, as in benzodiazepine-withdrawn rodents associated with signs of physical dependence (Katsura *et al*, 2007; Xiang *et al*, 2008), cocaine sensitization was also associated with an enhancement of Ca^{2+} entry through L-type voltage-gated Ca^{2+} channels (Nasif *et al*, 2005; Ford *et al*, 2009). Accordingly, the sources of Ca^{2+} entry during drug withdrawal, the resultant effect on CaMKIIα activation and, in turn AMPAR potentiation in specific brain areas might in part explain the differences detected among models of activity dependent and drug-induced plasticity. That is, upstream mechanisms of CaMKII activation may differ between models of activity-dependent plasticity resulting from brief, coincident activation of excitatory pathways, such as in LTP or fear-conditioning (McKernan and Shinnick-Gallagher, 1997; Rodrigues *et al*, 2004) in comparison to drug-induced plasticity resulting from more persistent, selective activation of drug targets in specific neural circuits.

Acknowledgments

We thank Krista Pettee, Brian Behrle, Margarete Otting and Eugene Orlowski for expert technical assistance. We would also like to acknowledge L. J. Greenfield, Jr. M.D. Ph.D. for critically reading the final manuscript. This work was supported by Department of Health and Human Services Grant R01-DA18342 from the National Institute on Drug Abuse (NIDA) to E.I.T.; an individual predoctoral NRSA grant F30-DA06041 from NIDA to BJV; and predoctoral fellowships from the University of Toledo College of Medicine Biomedical Sciences Graduate Program (to GS, BJV and MM). The National Institute of Drug Abuse Drug Supply Program supplied flurazepam.

References

Adesnik H, Nicoll RA. Conservation of glutamate receptor 2-containing AMPA receptors during long-term potentiation. J Neurosci. 2007; 27:4598–4602. [PubMed: 17460072]

Anderson SM, Famous KR, Sadri-Vakili G, Kumaresan V, Schmidt HD, Bass CE, Terwilliger EF, Cha JH, Pierce RC. CaMKII: a biochemical bridge linking accumbens dopamine and glutamate systems in cocaine seeking. Nat Neurosci. 2008; 11:344–53. [PubMed: 18278040]

Allison C, Pratt JA. Neuroadaptive processes in GABAergic and glutamatergic systems in benzodiazepine dependence. Pharmacol Ther. 2003; 98:171–195. [PubMed: 12725868]

Barria A, Derkach V, Soderling T. Identification of the Ca^{2+}/calmodulin-dependent protein kinase II regulatory phosphorylation site in the alpha-amino-3-hydroxyl-5-methyl-4-isoxazole-propionate-type glutamate receptor. J Biol Chem. 1997a; 272:32727–32730. [PubMed: 9407043]

Barria A, Muller D, Derkach V, Griffith LC, Soderling TR. Regulatory phosphorylation of AMPA-type glutamate receptors by CaM-KII during long-term potentiation. Science. 1997b; 276:2042–2045. [PubMed: 9197267]

Bateson AN. Basic pharmacologic mechanisms involved in benzodiazepine tolerance and withdrawal. Curr Pharm Des. 2002; 8:5–21. [PubMed: 11812247]

Bayer KU, De Koninck P, Leonard AS, Hell JW, Schulman H. Interaction with the NMDA receptor locks CaMKII in an active conformation. Nature. 2001; 411:801–805. [PubMed: 11459059]

Bayer KU, LeBel E, McDonald GL, O'Leary H, Schulman H, De Koninck P. Transition from reversible to persistent binding of CaMKII to postsynaptic sites and NR2B. J Neurosci. 2006; 26:1164–1174. [PubMed: 16436603]

Benke TA, Luthi A, Isaac JT, Collingridge GL. Modulation of AMPA receptor unitary conductance by synaptic activity. Nature. 1998; 393:793–797. [PubMed: 9655394]

Boudreau AC, Ferrario CR, Glucksman MJ, Wolf ME. Signaling pathway adaptations and novel protein kinase A substrates related to behavioral sensitization to cocaine. J Neurochem. 2009; 110:363–377. [PubMed: 19457111]

Boudreau AC, Wolf ME. Behavioral sensitization to cocaine is associated with increased AMPA receptor surface expression in the nucleus accumbens. J Neurosci. 2005; 25:9144–9151. [PubMed: 16207873]

Collingridge GL, Olsen RW, Peters J, Spedding M. A nomenclature for ligand-gated ion channels. Neuropharmacology. 2009; 56:2–5. [PubMed: 18655795]

Collingridge GL, Isaac JT, Wang YT. Receptor trafficking and synaptic plasticity. Nat Rev Neurosci. 2004; 5:952–962. [PubMed: 15550950]

Das P, Lilly SM, Zerda R, Gunning WT 3rd, Alvarez FJ, Tietz EI. Increased AMPA receptor GluR1 subunit incorporation in rat hippocampal CA1 synapses during benzodiazepine withdrawal. J Comp Neurol. 2008; 511:832–846. [PubMed: 18924138]

Das P, Zerda R, Alvarez FJ, Tietz EI. Immunogold electron microscopic evidence of differential regulation of GluN1, GluN2A and GluN2B, NMDA-type glutamate receptor subunits in rat hippocampal CA1 synapses during benzodiazepine withdrawal. J Comp Neurol. 2009 acceptable with minor revision.

Derkach V, Barria A, Soderling TR. Ca^{2+}/calmodulin-kinase II enhances channel conductance of alpha-amino-3-hydroxy-5-methyl-4-isoxazolepropionate type glutamate receptors. Proc Natl Acad Sci U S A. 1999; 96:3269–3274. [PubMed: 10077673]

Derkach VA, Oh MC, Guire ES, Soderling TR. Regulatory mechanisms of AMPA receptors in synaptic plasticity. Nat Rev Neurosci. 2007; 8:101–113. [PubMed: 17237803]

Dunworth SJ, Stephens DN. Sensitisation to repeated withdrawal, in mice treated chronically with diazepam, is blocked by an NMDA receptor antagonist. Psychopharmacology (Berl). 1998; 136:308–310. [PubMed: 9566818]

Edwards S, Graham DL, Whisler KN, Self DW. Phosphorylation of GluR1, ERK, and CREB during spontaneous withdrawal from chronic heroin self-administration. Synapse. 2009; 63:224–235. [PubMed: 19084907]

Esteban JA, Shi SH, Wilson C, Nuriya M, Huganir RL, Malinow R. PKA phosphorylation of AMPA receptor subunits controls synaptic trafficking underlying plasticity. Nat Neurosci. 2003; 6:136–143. [PubMed: 12536214]

Fitzgerald LW, Ortiz J, Hamedani AG, Nestler EJ. Drugs of abuse and stress increase the expression of GluR1 and NMDAR1 glutamate receptor subunits in the rat ventral tegmental area: Common adaptations among cross-sensitizing agents. J Neurosci. 1996; 16:274–82. [PubMed: 8613793]

Ford KA, Wolf ME, Hu XT. Plasticity of L-type Ca^{2+} channels after cocaine withdrawal. Synapse. 2009; 63:690–697. [PubMed: 19360908]

Gao L, Blair LA, Marshall J. CaMKII-independent effects of KN93 and its inactive analog KN92: reversible inhibition of L-type calcium channels. Biochem Biophys Res Commun. 2006; 345:1606–1610. [PubMed: 16730662]

Gebhardt C, Cull-Candy SG. Influence of agonist concentration on AMPA and kainate channels in CA1 pyramidal cells in rat hippocampal slices. J Physiol. 2006; 573:371–394. [PubMed: 16527860]

Ghasemzadeh MB, Mueller C, Vasudevan P. Behavioral sensitization to cocaine is associated with increased glutamate receptor trafficking to the postsynaptic density after extended withdrawal period. Neuroscience. 2009; 159:414–426. [PubMed: 19105975]

Glass MJ, Kruzich PJ, Colago EE, Kreek MJ, Pickel VM. Increased AMPA GluR1 receptor subunit labeling on the plasma membrane of dendrites in the basolateral amygdala of rats self-administering morphine. Synapse. 2005; 58:1–12. [PubMed: 16037950]

Glass MJ, Lane DA, Colago EE, Chan J, Schlussman SD, Zhou Y, et al. Chronic administration of morphine is associated with a decrease in surface AMPA GluR1 receptor subunit in dopamine D1 receptor expressing neurons in the shell and non-D1 receptor expressing neurons in the core of the rat nucleus accumbens. Exp Neurol. 2008; 210:750–761. [PubMed: 18294632]

Griffiths RR, Johnson MW. Relative abuse liability of hypnotic drugs: a conceptual framework and algorithm for differentiating among compounds. J Clin Psychiatry. 2005; 9(66):31–41. [PubMed: 16336040]

Guire ES, Oh MC, Soderling TR, Derkach VA. Recruitment of calcium-permeable AMPA receptors during synaptic potentiation is regulated by CaM-kinase I. J Neurosci. 2008; 28:6000–6008. [PubMed: 18524905]

Hayashi Y, Shi SH, Esteban JA, Piccini A, Poncer JC, Malinow R. Driving AMPA receptors into synapses by LTP and CaMKII: requirement for GluR1 and PDZ domain interaction. Science. 2000; 287:2262–2267. [PubMed: 10731148]

He K, Song L, Cummings LW, Goldman J, Huganir RL, Lee HK. Stabilization of Ca2+-permeable AMPA Receptor at perisynaptic sites by GluR1-S845 phosphorylation. Proc Natl Acad Sci U S A. 2009; 106:20033–20038. [PubMed: 19892736]

Hollmann M, Hartley M, Heinemann S. Ca^{2+} permeability of KA-AMPA--gated glutamate receptor channels depends on subunit composition. Science. 1991; 252:851–853. [PubMed: 1709304]

Ishida A, Kameshita I, Okuno S, Kitani T, Fujisawa H. A novel highly specific and potent inhibitor of calmodulin-dependent protein kinase II. Biochem Biophys Res Commun. 1995; 212:806–812. [PubMed: 7626114]

Izzo E, Auta J, Impagnatiello F, Pesold C, Guidotti A, Costa E. Glutamic acid decarboxylase and glutamate receptor changes during tolerance and dependence to benzodiazepines. Proc Natl Acad Sci U S A. 2001; 98:3483–3488. [PubMed: 11248104]

Katsura M, Shibasaki M, Kurokawa K, Tsujimura A, Ohkuma S. Up-regulation of L-type high voltage-gated calcium channel subunits by sustained exposure to 1,4- and 1,5-benzodiazepines in cerebrocortical neurons. J Neurochem. 2007; 103:2518–2528. [PubMed: 17949410]

Kauer JA, Malenka RC. Synaptic plasticity and addiction. Nat Rev Neurosci. 2007; 8:844–858. [PubMed: 17948030]

Koff JM, Pritchard GA, Greenblatt DJ, Miller LG. The NMDA receptor competitive antagonist CPP modulates benzodiazepine tolerance and discontinuation. Pharmacology. 1997; 55:217–227. [PubMed: 9399331]

Lee HK, Takamiya K, He K, Song L, Huganir RL. Specific roles of AMPA receptor subunit GluR1 (GluA1) phosphorylation sites in regulating synaptic plasticity in the CA1 region of hippocampus. J Neurophysiol. 2010; 103:479–89. [PubMed: 19906877]

Lerma J, Morales M, Ibarz JM, Somohano F. Rectification properties and Ca^{2+} permeability of glutamate receptor channels in hippocampal cells. Eur J Neurosci. 1994; 6:1080–1088. [PubMed: 7524964]

Lisman J, Schulman H, Cline H. The molecular basis of CaMKII function in synaptic and behavioural memory. Nat Rev Neurosci. 2002; 3:175–190. [PubMed: 11994750]

Lledo PM, Hjelmstad GO, Mukherji S, Soderling TR, Malenka RC, Nicoll RA. Calcium/calmodulin-dependent kinase II and long-term potentiation enhance synaptic transmission by the same mechanism. Proc Natl Acad Sci U S A. 1995; 92:11175–11179. [PubMed: 7479960]

Llinas R, McGuinness TL, Leonard CS, Sugimori M, Greengard P. Intraterminal injection of synapsin I or calcium/calmodulin-dependent protein kinase II alters neurotransmitter release at the squid giant synapse. Proc Natl Acad Sci U S A. 1985; 82:3035–3039. [PubMed: 2859595]

Loweth JA, Singer BF, Baker LK, Wilke G, Inamine H, Bubula N, Alexander JK, Carlezon WA Jr, Neve RL, Vezina P. Transient overxpression of alpha-Ca^{2+}/calmodulin-dependent protein kinase II in the nucleus accumbens shell enhances behavioral responding to amphetamine. J Neurosci. 2010; 30:939–949. [PubMed: 20089902]

Lu W, Shi Y, Jackson AC, Bjorgan K, During MJ, Sprengel R, Seeburg PH, Nicoll RA. Subunit composition of synaptic AMPA receptors revealed by a single-cell genetic approach. Neuron. 2009; 62:254–268. [PubMed: 19409270]

Luthi A, Wikstrom MA, Palmer MJ, Matthews P, Benke TA, Isaac JT, et al. Bi-directional modulation of AMPA receptor unitary conductance by synaptic activity. BMC Neurosci. 2004; 5:44. [PubMed: 15538948]

Mammen AL, Kameyama K, Roche KW, Huganir RL. Phosphorylation of the alpha-amino-3-hydroxy-5-methylisoxazole4-propionic acid receptor GluR1 subunit by calcium/calmodulin-dependent kinase II. J Biol Chem. 1997; 272:32528–32533. [PubMed: 9405465]

Margrie TW, Rostas JA, Sah P. Presynaptic long-term depression at a central glutamatergic synapse: a role for CaMKII. Nat Neurosci. 1998; 1:378–383. [PubMed: 10196527]

McKernan MG, Shinnick-Gallagher P. Fear conditioning induces a lasting potentiation of synaptic currents in vitro. Nature. 1997; 390:607–611. [PubMed: 9403689]

Moga DE, Janssen WG, Vissavajjhala P, Czelusniak SM, Moran TM, Hof PR, et al. Glutamate receptor subunit 3 (GluR3) immunoreactivity delineates a subpopulation of parvalbumin-containing interneurons in the rat hippocampus. J Comp Neurol. 2003; 462:15–28. [PubMed: 12761821]

Nasif FJ, Hu XT, White FJ. Repeated cocaine administration increases voltage-sensitive calcium currents in response to membrane depolarization in medial prefrontal cortex pyramidal neurons. J Neurosci. 2005; 25:3674–3679. [PubMed: 15814798]

Nicoll RA. Expression mechanisms underlying long-term potentiation: a postsynaptic view. Philos Trans R Soc Lond B Biol Sci. 2003; 358:721–726. [PubMed: 12740118]

Oh MC, Derkach VA. Dominant role of the GluR2 subunit in regulation of AMPA receptors by CaMKII. Nat Neurosci. 2005; 8:853–854. [PubMed: 15924137]

Ortiz J, Fitzgerald LW, Charlton M, Lane S. Biochemical actions of chronic ethanol exposure in the mesolimbic dopamine system. Synapse. 1995; 21:289–298. [PubMed: 8869159]

Pellegrini-Giampietro DE. An activity-dependent spermine-mediated mechanism that modulates glutamate transmission. Trends Neurosci. 2003; 26:9–11. [PubMed: 12495855]

Plant K, Pelkey KA, Bortolotto ZA, Morita D, Terashima A, McBain CJ, et al. Transient incorporation of native GluR2-lacking AMPA receptors during hippocampal long-term potentiation. Nat Neurosci. 2006; 9:602–604. [PubMed: 16582904]

Poncer JC, Esteban JA, Malinow R. Multiple mechanisms for the potentiation of AMPA receptor-mediated transmission by alpha-Ca^{2+}/calmodulin-dependent protein kinase II. J Neurosci. 2002; 22:4406–4411. [PubMed: 12040047]

Rodrigues SM, Schafe GE, LeDoux JE. Molecular mechanisms underlying emotional learning and memory in the lateral amygdala. Neuron. 2004; 44:75–91. [PubMed: 15450161]

Sanhueza M, McIntyre CC, Lisman JE. Reversal of synaptic memory by Ca^{2+}/calmodulin-dependent protein kinase II inhibitor. J Neurosci. 2007; 27:5190–5199. [PubMed: 17494705]

Sans N, Vissel B, Petralia RS, Wang YX, Chang K, Royle GA, et al. Aberrant formation of glutamate receptor complexes in hippocampal neurons of mice lacking the GluR2 AMPA receptor subunit. J Neurosci. 2003; 23:9367–9373. [PubMed: 14561864]

Seeburg PH. The role of RNA editing in controlling glutamate receptor channel properties. J Neurochem. 1996; 66:1–5. [PubMed: 8522940]

Shen H, Gong QH, Aoki C, Yuan M, Ruderman Y, Dattilo M, et al. Reversal of neurosteroid effects at alpha4beta2delta $GABA_A$ receptors triggers anxiety at puberty. Nat Neurosci. 2007; 10:469–477. [PubMed: 17351635]

Shen, G.; Tietz, EI. Regulation of synaptic NR2B subunit-containing NMDA receptors: one component of glutamatergic plasticity in benzodiazepine withdrawal-anxiety. Soc Neurosci Abstr; Program # 662, Neuroscience Meeting Planner; Washington DC: Society for Neuroscience. 2008; 2008. Online

Shen G, Van Sickle BJ, Tietz EI. Positive allosteric activation of $GABA_A$ receptors bi-directionally modulates hippocampal glutamate plasticity and behavior. Biochem Soc Trans. 2009; 37:1394–1398. [PubMed: 19909283]

Shen K, Teruel MN, Subramanian K, Meyer T. CaMKIIbeta functions as an F-actin targeting module that localizes CaMKIIalpha/beta heterooligomers to dendritic spines. Neuron. 1998; 21:593–606. [PubMed: 9768845]

Shi SH, Hayashi Y, Petralia RS, Zaman SH, Wenthold RJ, Svoboda K, et al. Rapid spine delivery and redistribution of AMPA receptors after synaptic NMDA receptor activation. Science. 1999; 284:1811–1816. [PubMed: 10364548]

Song, J.; Tietz, EI. AMPA receptor plasticity in benzodiazepine-withdrawn rats is associated with only a transient increase in GluR1 subunit Ser^{845} phosphorylation in hippocampal CA1 neurons. Soc Neurosci Abstr; Program No 511.5, Neuroscience Meeting Planner; San Diego, CA: Society for Neuroscience. 2004; 2004. Online

Song J, Shen G, Greenfield LJ Jr, Tietz EI. Benzodiazepine withdrawal-induced glutamatergic plasticity involves up-regulation of GluR1-containing alpha-amino-3-hydroxy-5-methylisoxazole-4-propionic acid receptors in Hippocampal CA1 neurons. J Pharmacol Exp Ther. 2007; 322:569–581. [PubMed: 17510319]

Spruston N, Jonas P, Sakmann B. Dendritic glutamate receptor channels in rat hippocampal CA3 and CAl pyramidal neurons. J Physiol. 1995; 482:325–352. [PubMed: 7536248]

Sutton MA, Schmidt EF, Choi KH, Schad CA, Whisler K, Simmons D, Karanian DA, Monteggia LM, Neve RL, Self DW. Extinction-induced upregulation in AMPA receptors reduces cocaine-seeking behaviour. Nature. 2003; 421:70–75. [PubMed: 12511956]

Swanson GT, Kamboj SK, Cull-Candy SG. Single-channel properties of recombinant AMPA receptors depend on RNA editing, splice variation, and subunit composition. J Neurosci. 1997; 17:58–69. [PubMed: 8987736]

Van Sickle BJ, Cox AS, Schak K, Greenfield LJ Jr, Tietz EI. Chronic benzodiazepine administration alters hippocampal CA1 neuron excitability: NMDA receptor function and expression(1). Neuropharmacology. 2002; 43:595–606. [PubMed: 12367605]

Van Sickle BJ, Tietz EI. Selective enhancement of AMPA receptor-mediated function in hippocampal CA1 neurons from chronic benzodiazepine-treated rats. Neuropharmacology. 2002; 43:11–27. [PubMed: 12213255]

Van Sickle BJ, Xiang K, Tietz EI. Transient plasticity of hippocampal CA1 neuron glutamate receptors contributes to benzodiazepine withdrawal-anxiety. Neuropsychopharmacology. 2004; 29:1994–2006. [PubMed: 15266351]

Wafford KA. GABA-A receptor subtypes: any clues to the mechanism of benzodiazepine dependence? Curr Opin Pharmacol. 2005; 5:47–52. [PubMed: 15661625]

Wang JH, Kelly PT. Postsynaptic injection of Ca^{2+}/CaM induces synaptic potentiation requiring CaMKII and PKC activity. Neuron. 1995; 15:443–452. [PubMed: 7646896]

Washburn MS, Dingledine R. Block of alpha-amino-3-hydroxy-5-methyl-4-isoxazolepropionic acid (AMPA) receptors by polyamines and polyamine toxins. J Pharmacol Exp Ther. 1996; 278:669–678. [PubMed: 8768718]

Wenthold RJ, Petralia RS, Blahos J II, Niedzielski AS. Evidence for multiple AMPA receptor complexes in hippocampal CA1/CA2 neurons. J Neurosci. 1996; 16:1982–1989. [PubMed: 8604042]

Wolf ME, Sun X, Mangiavacchi S, Chao SZ. Psychomotor stimulants and neuronal plasticity. Neuropharmacology. 47:61–79. [PubMed: 15464126]

Xiang K, Tietz EI. Benzodiazepine-induced hippocampal CA1 neuron alpha-amino-hydroxy-5-methylisoxasole-4-propionic acid (AMPA) receptor plasticity linked to severity of withdrawal anxiety: Differential role of voltage-gated calcium channels and N-methyl-D-aspartic acid receptors. Behav Pharmacol. 2007; 18:447–460. [PubMed: 17762513]

Xiang K, Earl DE, Davis K, Giovannucci DR, Greenfield LJ Jr, Tietz EI. Chronic benzodiazepine administration potentiates high voltage-activated calcium currents in hippocampal CA1 neurons. J Pharmacol Exp Ther. 2008; 327:872–883. [PubMed: 18812492]

Zeng X, Tietz EI. Benzodiazepine tolerance at GABAergic synapses on hippocampal CA1 Pyramidal Cells. Synapse. 1999; 31:263–277. [PubMed: 10051107]

Zhu JJ, Esteban JA, Hayashi Y, Malinow R. Postnatal synaptic potentiation: delivery of GluA4-containing AMPA receptors by spontaneous activity. Nat Neurosci. 2000; 3:1098–1106. [PubMed: 11036266]

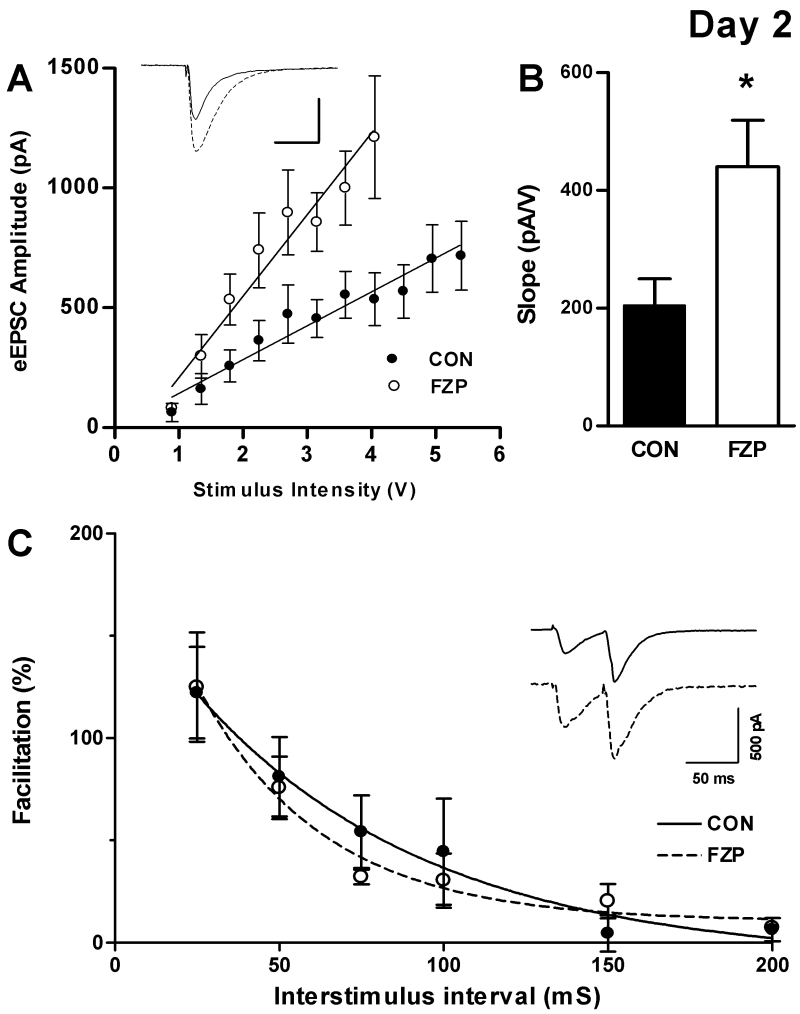

Fig 1.

The slope of the input–output (I/O) relationship, but not paired-pulse facilitation was increased in CA1 neurons from 2-day FZP-withdrawn rats. (A) Evoked EPSC (V_H = -80 mV) amplitude (pA) was plotted as a function of stimulus intensity (V). Linear regression of pooled I/O relationships showed a ∼2.5 fold increase in the stimulus response relationship in CA1 neurons from FZP-withdrawn (open circles, n=9) compared to control (closed circles, n=7) rats. Inset: Representative traces of eEPSCs elicited at 3.6V (solid line: CON; broken line: FZP). Scale as in inset in C. (B) The mean slope of the I/O curve derived from the fits of individual I/O curves generated in neurons from FZP-withdrawn rats (440.0 ± 79.4 pA/V, n=9) was also significantly greater than that from control rats (205.3 ± 44.5 pA/V, n=7). The data are consistent with an increase in CA1 neuron AMPAR synaptic efficacy in FZP-withdrawn rats. Asterisks denote $p<.05$. (C) Paired-pulse facilitation (PPF) of AMPAR was unchanged in 2-day FZP withdrawn rats. The amplitude of AMPAR-mediated eEPSCs (V_H = -80 mV) following half-maximal stimulation of the Schaffer-collateral pathway. Paired-pulse stimulation was applied and the response was recorded at the inter-stimulus intervals ranging from 25-200 ms in 25 ms increments. Inset: Representative paired EPSC traces recorded in CA1 neurons from control and FZP-

withdrawn rats. Paired EPSC amplitudes were calculated as the difference between baseline before the stimulus artifact and EPSC peak. PPF was calculated as (EPSC2-EPSC1)/EPSC1 × 100. Percent facilitation was plotted (CON, closed circles, n = 5; FZP: closed circles, n = 5) and fit with a single exponential decay function. No significant differences between groups were found at any interstimulus interval suggesting that glutamate release onto CA1 neurons was unaltered.

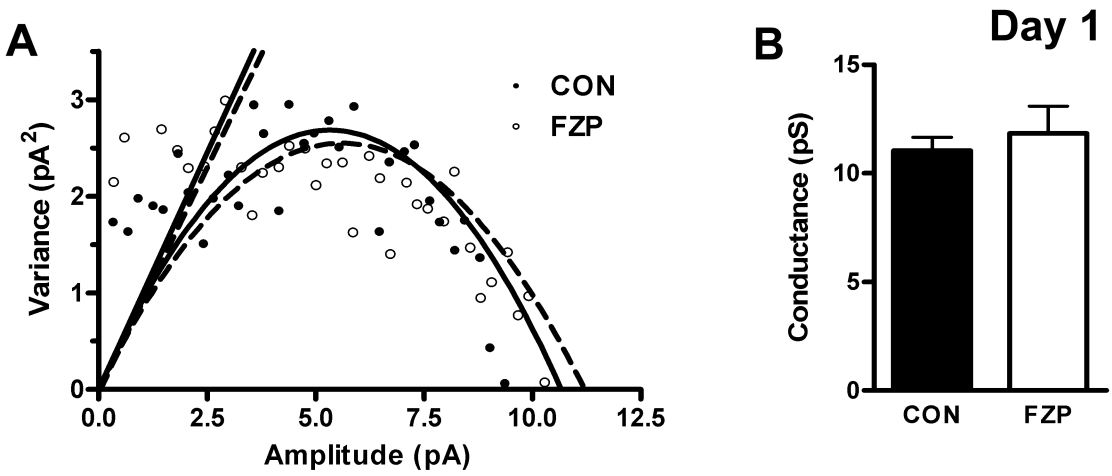

Fig 2.

AMPAR-mediated mEPSC amplitude, but not conductance was increased in 1-day FZP-withdrawn rats. mEPSC amplitude was increased in 1-day FZP withdrawn rats without an effect on mEPSC frequency, rise-time or decay kinetics, or RMP. (A) Representative plot of the results of non-stationary noise analysis (NSNA) of mEPSCs showed an increase in current amplitude, but no change in slope conductance in a FZP-withdrawn (open circles/ dotted line) versus a CON (close circles/solid line) neuron. (B) Mean mEPSC conductance in CA1 neurons from CON (closed bars, n= 6) and 1-day FZP-withdrawn (open bars, n= 7) rats indicated no significant difference in AMPAR conductance between experimental groups at this time-point.

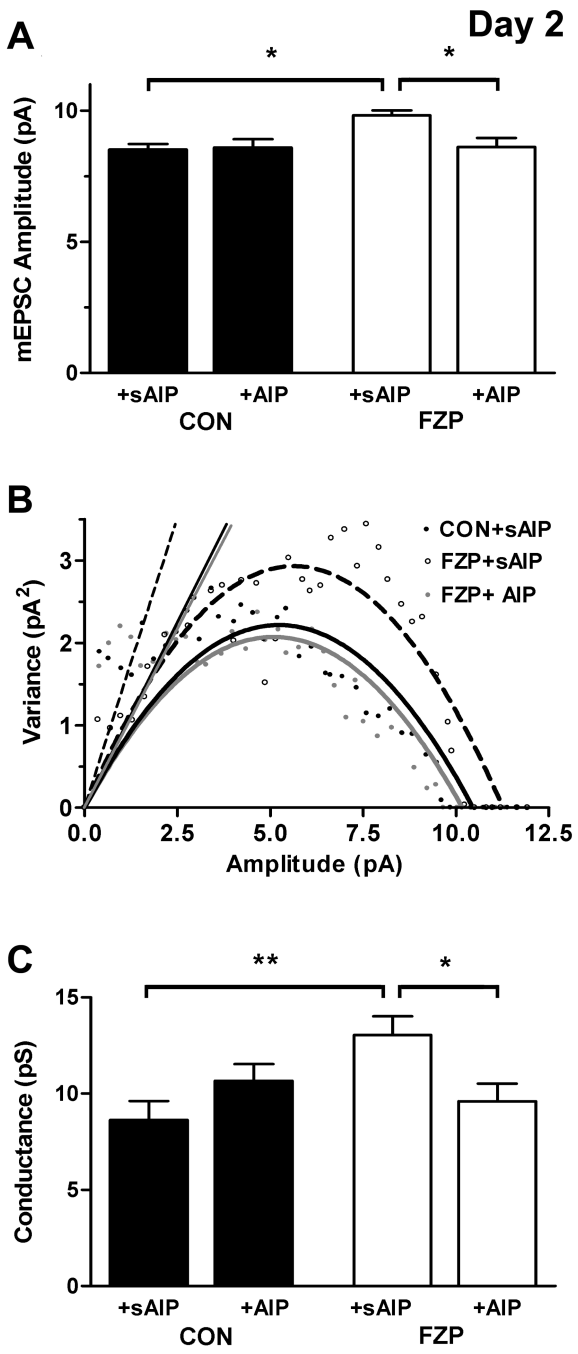

Fig 3.

Both AMPAR amplitude and single-channel conductance was reversed by intracellular inclusion of a CaMKII inhibitor. As recorded in ACSF alone (Shen *et al.*, 2009) and as shown in Table 1, mEPSC (A) amplitude and (C) conductance were significantly increased in 2-day FZP-withdrawn rats in the negative control condition, with scrambled autocamtide inhibitory peptide (sAIP) in the whole-cell micropipette. (B) Representative plot of the results of NSNA of mEPSCs showing an increased current amplitude and slope conductance in an FZP-withdrawn neuron with sAIP (open circles/dotted line) versus a CON neuron with

sAIP (close circles/black solid line). Intracellular inclusion of the active CaMKII inhibitor, +AIP reversed both the increased AMPAR-mediated mEPSC (A) amplitude and (C) elevated single-channel conductance to control levels (+sAIP) as illustrated in (B) (grey circles/grey solid line). CaMKIINtide inclusion in a few neurons had a similar effect, suggesting that AMPAR potentiation is mediated by CaMKIIα activation.

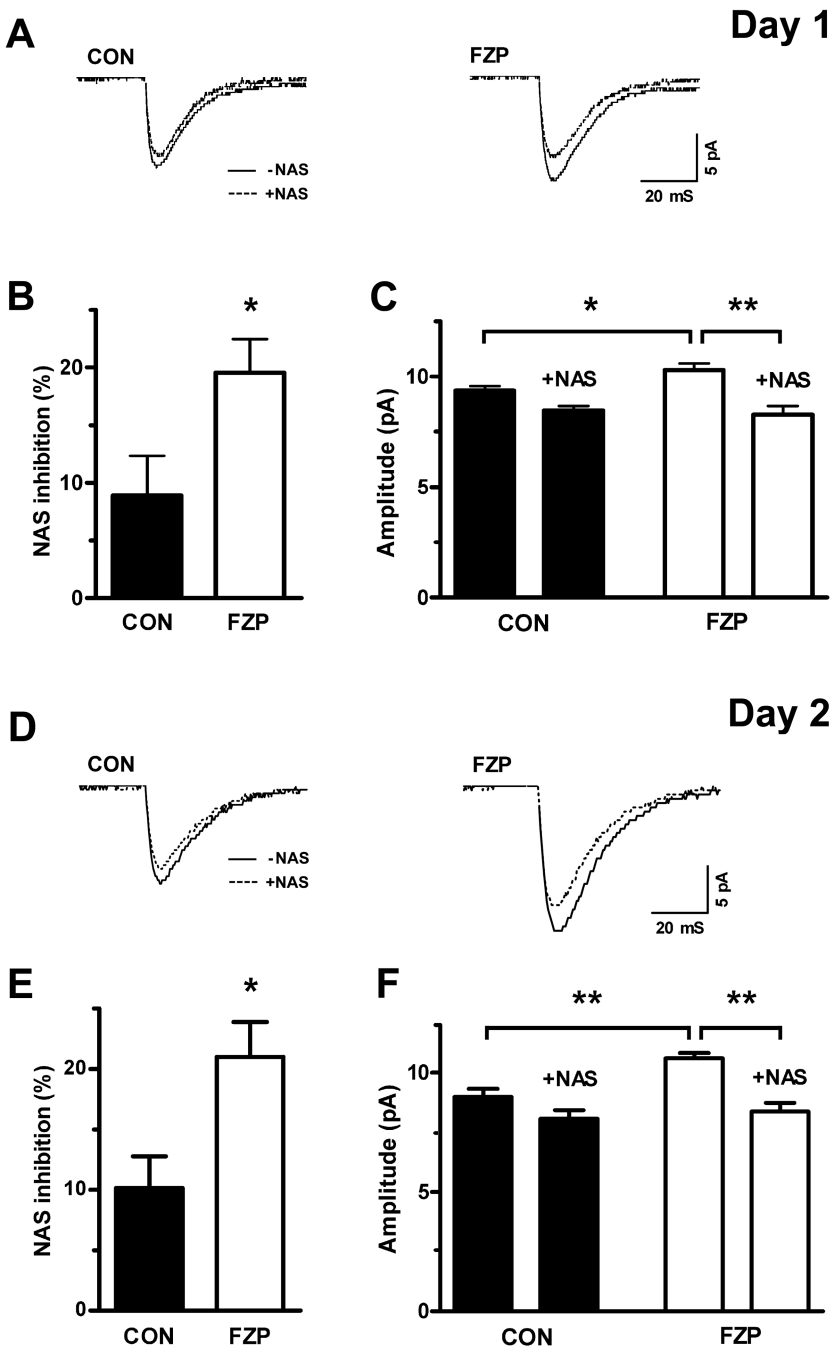

Fig 4.

Greater NAS inhibition in neurons from 1- and 2-day FZP-withdrawn rats. Representative AMPAR-mediated mEPSCs (A, 1-day; D, 2-day) recorded before (solid line) and after (dotted line) external application of the potent spermine analogue, NAS (100 μM). The percent NAS inhibition of mEPSC current amplitude was increased (B, 1-day; E, 2-day) in CA1 neurons from FZP-withdrawn rats ($p<0.05$). Bath application of NAS abolished the increased AMPAR-mediated mEPSC amplitude in FZP-withdrawn neurons after 1-day (n= 7) and 2-days (n=12) and was without effect in control neurons (1-day, n= 6; 2-days, n=7),

supporting the hypothesis that AMPAR current potentiation is mediated by synaptic incorporation of GluA2-lacking AMPARs. Asterisks denote * p≤.05 or ** p≤.01.

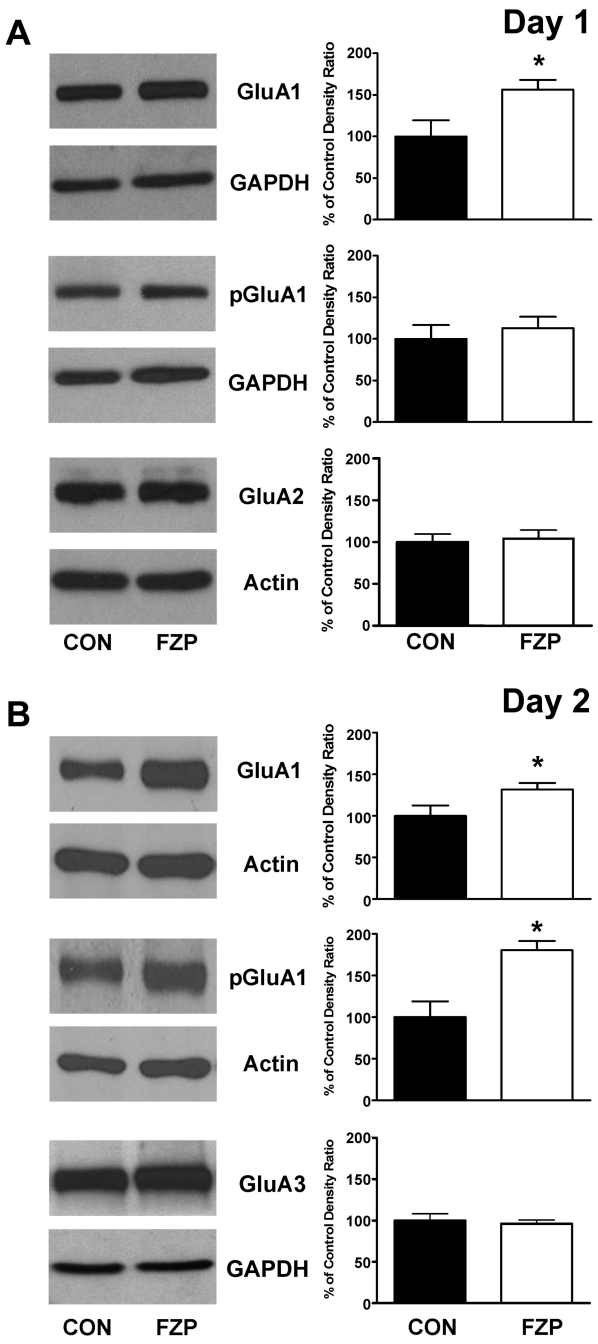

Fig 5.

GluA subunit levels in CA1 PSD-enriched subcellular fractions as a function of time after drug withdrawal. PSD-enriched subfractions were collected by ultracentrifugation of TritonX-100-resistant membranes pooled from 3 hippocampal CA1 minislices as described in the methods. Representative immunoblots of total GluA1 and pSer^{831}GluA1 with their respective loading controls are shown in PSD-enriched subfractions from (A) 1-day and (B) 2-day FZP-withdrawn rats in the leftmost panels. Histograms of integrated signal density as a percent of paired control density (n=4-11 lanes/group) are shown to the right. Only total-

GluA1 expression levels were significantly enhanced in 1-day FZP withdrawn rats, while both total and pSer^{831}GluA1 levels were increased in 2-day FZP withdrawn rats. There were no changes in GluA2 levels in 1-day (or 2-day, Das *et al*, 2008; Song *et al*, 2007) FZP-withdrawn rats. There were also no changes in GluA3 expression levels in the PSD-enriched fraction from 2-day FZP withdrawn rats. Asterisks denote $p<.05$.

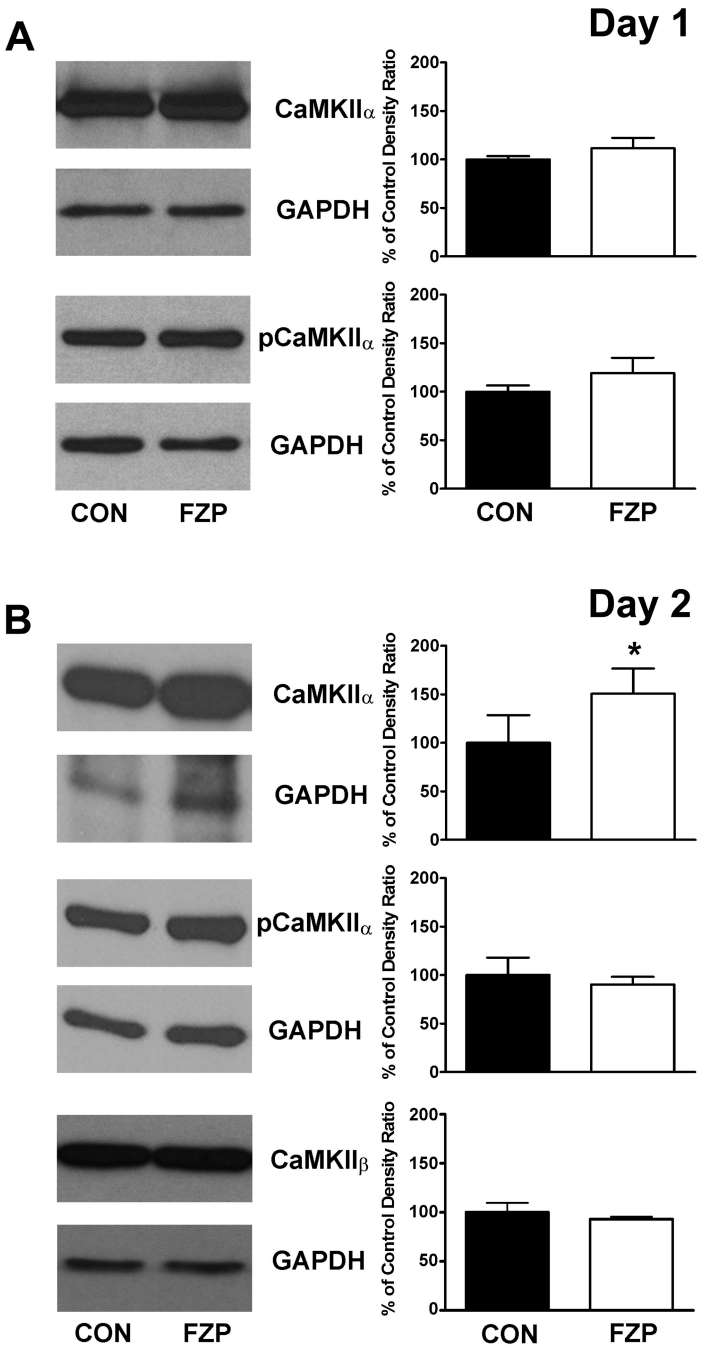

Fig 6.

CaMKII subunit levels in CA1 PSD-enriched subcellular fractions as a function of time after drug withdrawal. Representative immunoblots of total CaMKIIα, pThr^{286}-CaMKIIα and CaMKIIβ protein with their respective GAPDH loading controls are shown in PSD-enriched subfractions of CA1 minislices from (A) 1-day and (B) 2-day FZP-withdrawn rats in the leftmost panels. Histograms of integrated signal density as a percent of the paired control density (n=4-7 lanes/group) are shown to the right. Total-CaMKIIα expression levels were

significantly increased in 2-day FZP-withdrawn rats. No significant changes in pThr^{286}-CaMKIIα or CaMKIIβ expression levels were found. Asterisks denote $p<.05$.

Table 1

mEPSC characteristics after postsynaptic application of CaMKII inhibitors

Group (# cells)	RMP (mV)	Frequency (Hz)	Rise time (ms)	Amplitude (pA)	Decay tau (ms)	Conductance (pS)
CON						
+sAIP (n = 7)	-68.3 ± 1.0	0.23 ± 0.03	3.6 ± 0.3	-8.5 ± 0.2	19.5 ± 1.6	8.6 ± 1.0
+ AIP (n = 6)	-66.0 ± 1.4	0.40 ± 0.09	2.9 ± 0.2	-8.6 ± 0.3	18.2 ± 1.1	10.7 ± 0.9
+ACM (n = 7)	-65.6 ± 1.9	0.30 ± 0.09	3.0 ± 0.2	-8.7 ± 0.2	17.8 ± 0.9	10.4 ± 0.4
FZP						
+sAIP (n = 7)	-64.7 ± 1.4	0.35 ± 0.10	3.0 ± 0.2	-9.8 ± 0.2*	17.0 ± 0.6	13.0 ± 1.0**
+ AIP (n = 8)	-67.6 ± 1.9	0.37 ± 0.09	3.2 ± 0.2	-8.6 ± 0.4†	19.5 ± 1.5	9.6 ± 0.9
+ACM (n = 9)	-67.1 ± 2.3	0.27 ± 0.03	3.2 ± 0.1	-9.3 ± 0.3	17.4 ± 1.4	10.8 ± 0.6

Values are listed as means ± S.E.M.

** p<0.01;

* p<0.05 (CON+sAIP vs. FZP+sAIP);

$^{\dagger *}$ p<0.05 (FZP+sAIP vs. FZP+AIP)